Vibrational Analysis of Methylcobalamin

Tadeusz Andruniow,[†] Marek Z. Zgierski,[‡] and Pawel M. Kozlowski*,[†]

Department of Chemistry, University of Louisville, Louisville, Kentucky 40292, and Steacie Institute for Molecular Science, National Research Council of Canada, Ottawa, Ontario, Canada K1A OR6

Received: August 3, 2001; In Final Form: December 4, 2001

This work represents the first theoretical attempt to assign vibrational modes for methylcobalamin (MeCbl), the biologically active form of a vitamin B_{12} derivative. Full vibrational analysis of MeCbl is currently beyond computational resources; thus, a simplified model, including the actual corrin ring, Im−[Co^{III}(corrin)]−CH_3, was employed in the analysis. The scaled quantum mechanical (SQM) method has been used to refine density functional theory (DFT) based force constants calculated at the B3LYP level of theory. Normal-coordinate analysis based on a six-coordinate MeCbl model permitted assignment of the most important interligand modes. Direct comparison with experimental data showed that the DFT-SQM force field accurately predicts isotope shifts for interligand vibrations corresponding to $CH_3 \rightarrow CD_3$ and $^{12}CH_3 \rightarrow {}^{13}CH_3$ isotope labeling. The DFT-SQM force field for Im−[Co^{III}(corrin)]−CH_3 gives a semiquantitative description of the corrin modes when compared to the Raman spectrum of MeCbl. The analysis of Raman data, together with DFT-computed frequencies, permitted assignment of certain modes located in the 1300−1600 cm^{-1} range. The calculated modes in this spectral range are mainly composed of single/double CC and CN stretch vibrations. These modes more closely resemble vibrations of connected short linear polyenes rather than modes delocalized over the corrin ring as observed in porphyrins. This localized character most likely is responsible for lack of structure-sensitive modes such as the "core size" marker.

Introduction

Enzymes employing derivatives of vitamin B_{12} as a cofactor have long intrigued chemists because they carry out unusual molecular transformations with the aid of organometallic chemistry.[1] There are two classes of B_{12}-dependent enzymes: those using 5′-deoxy-5′-adenosyl-cobalamin [AdoCbl] and those using methylcobalamin [MeCbl] (Figure 1). The former catalyzes carbon-skeleton rearrangements[2] or ribonucleotide reduction,[3] while the latter is involved in methyl transfer reactions.[4] Elucidating these transformations has been the subject of active bioinorganic research and has been pursued with a variety of biophysical techniques. While intense interest continues in pursuing the mechanistic details of B_{12}-dependent enzymes which contain a cobalt corrinoid macrocycle (Figure 1) reminiscent of the more common heme prosthetic group, progress lags behind the impressive strides made in the study of heme proteins.[5] In fact, one of the most powerful spectroscopic probes of biologically relevant metallomacrocycles, resonance Raman (RR) spectroscopy, which has played a major role in revealing intricate active-site structural details of the heme enzymes and their catalytic intermediates, has not yet been fully utilized. RR spectroscopy is potentially an ideal probe for the active site structure of enzymes containing B_{12} as a cofactor because it is capable of monitoring Co−alkyl modes.[6] These modes modulate the corrin $\pi \rightarrow \pi^*$ transitions which dominate the visible absorption spectra via orbital interaction with the cobalt atom and can also provide information about the corrin conformation from vibrations of the corrin ring and the substituents. The extensive application of RR to B_{12}-dependent enzymes has been hampered mainly for two reasons. First of all, from an experimental perspective, RR spectroscopy has been hindered by the Co−C_R bond photolysis induced by the laser excitation. However, these difficulties associated with the Co−C_R bond scission have been recently overcome by using cryogenic techniques to prevent photolysis.[7] Using this technique, Spiro and co-workers were able to record spectra in situ in B_{12}-dependent enzymes.[8]

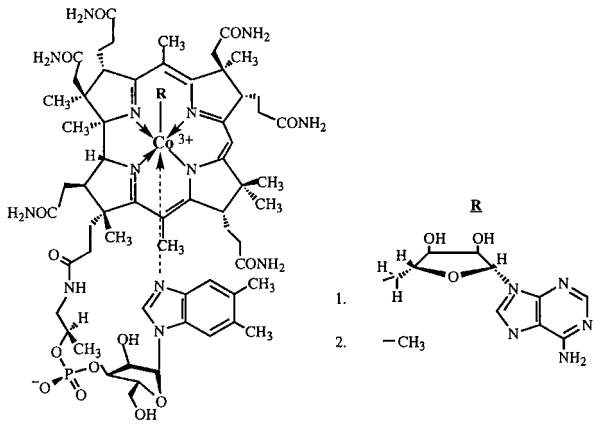

Figure 1. Molecular structure of (1) 5′-deoxy-5′-adenosylcobalamin [coenzyme B_{12}] and (2) methylcobalamin [CH_3Cbl].

A second major challenge in the spectroscopic characterization of B_{12}-dependent enzymes is the lack of a theoretical framework for assignment of vibrational frequencies, which hinders a meaningful structural interpretation of observed spectral changes. The fact that cobalamins lack any symmetry results in high complexity of their vibrational spectra. Consequently, only a few modes of cobalamin vibrational spectra have been assigned via isotopic substitution. Mainly, the Co−C_R

* Corresponding author. Phone: (502) 852-6609. Fax: (502) 852-8149. E-mail: pawel@louisville.edu.
[†] University of Louisville, Louisville,.
[‡] National Research Council of Canada.

10.1021/jp013271k CCC: $22.00
Published on Web 01/29/2002

TABLE 1: Calculated and Experimental Co−CH_3 Interligand Fundamental Frequencies (cm^{-1}), and Intensities [$(4\pi\epsilon_o)^2$ Å amu-1] of Im−[Co^{III}−corrin]−CH_3 and −CD_3 Isotopomer

Im−[Co^{III}−corrin]−CH_3[a]		CH_3Cbl experiment	Im−[Co^{III}−corrin]−CD_3[a]		CD_3Cbl experiment	
freq.	Raman intensity	freq.	Δ	Raman intensity	Δ	mode description
115	0.3		30	0.0		Co−CH_3 torsion
123	0.2		2[g]	0.4		Co−N_B stretch
(184, 202)[b]	(2.2, 1.6)		(10, 5)	(2.1, 1.2)		Co−CH_3 wagging
(281, 314)[b]	(2.1, 2.5)		(6, 5)	(2.2, 2.1)		Co−CH_3 wagging
512	33.6	506,[c] 504,[d] 500[e]	32, [12][f]	25.9	28,[c] 30,[e] [12][c,f]	Co−C_R stretch
(770, 779)[b]	(3.0, 4.6)	790[c]	(186,187)	(3.9, 2.5)	196[c]	CH_3 rocking
1189	22.7	1155	277	9.0	273	CH_3 sym. deformation

[a] Present work, nonlocal DFT calculations with B3LYP functional. [b] Pseudodegenerate pair of vibrations in Co−C_{10} and C_5−Co−C_{15} directions (see Figure 2 for atomic labeling). [c] Ref 7b. [d] Ref 9b. [e] Ref 9a. [f] $^{12}CH_3 \rightarrow {}^{13}CH_3$ isotope shift. [g] $^{14}N_B \rightarrow {}^{15}N_B$ isotope shift.

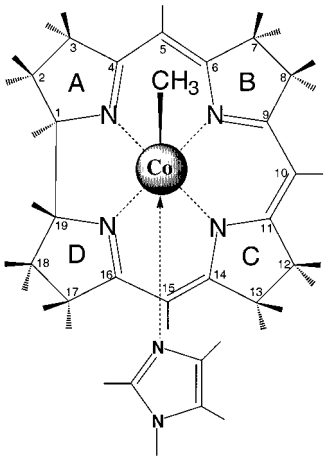

Figure 2. Molecular structure of Im−[Co^{III}−corrin]−CH_3 model.

stretches for MeCbl, EtCbl, and AdoCbl have been found at 506, 472, and 443/429 cm^{-1}, respectively,[7,9] and suggestions have been made about several modes occurring at ∼1500, ∼1545, ∼1570, and ∼1600 cm^{-1} associated with the corrin vibrations.[7b,9b,10,11] In this paper (and subsequent publications[12]), we address this issue computationally using density functional theory (DFT). We plan to remedy this situation by developing a quantitative vibrational force field (FF) for cobalt corrinoids capable of modeling vibrational spectra of B_{12}. To obtain a high-quality ground-state vibrational FF, we will follow the procedure developed by Pulay and co-workers referred as the scaled quantum mechanical (SQM) method.[13] The SQM method will be used to refine DFT-based force constants and to correct for possible systematic errors due to basis set truncation and incomplete treatment of electron correlation.

Results and Discussion

In this paper, we concentrate on a simplified model of methylcobalamin [MeCbl] shown in Figure 2. The full vibrational analysis of MeCbl is currently beyond available computational resources because of the size of the system. The simplified six-coordinate model of MeCbl, denoted as Im−[Co^{III}(corrin)]−CH_3, includes the actual corrin macrocycle ring as the equatorial ligand system and imidazole (Im) and methyl group as the α trans and β axial ligands, respectively. The sidearm and peripheral substituents of the corrin ring (Figure 1) were left out to simplify the calculations while important structural features were retained (Figure 2). Calculations were carried out using gradient corrected DFT with the Becke−Lee−Yang−Parr composite exchange correlation functional (B3LYP) as implemented in the Gaussian98 suite of programs for electronic structure calculation.[14] The B3LYP level of theory with 6-31G (d) [for H, C, N] and Ahlrichs' VTZ[15] (for Co) basis sets, successfully used in previous calculations on metalloporphyrins[16] and cobalamins,[17] was employed in the present study.

All normal frequencies at the optimized geometry were real, showing that optimized structure of Im−[Co^{III}(corrin)−CH_3 (Figure 2) corresponds to a stable minimum. We calculated the Cartesian force constants at the optimized geometry and transformed them to natural internal coordinates.[18] The natural internal coordinates were automatically generated by the TX90 program[19] and manually augmented. To refine the calculated DFT force constants, we used SQM procedure and scaled the resulting force constants according to the formula $F_{ij}' = (\lambda_i\lambda_j)^{1/2}F_{ij}$.[20] DFT off-resonance Raman intensities were calculated by finite perturbation theory as numerical second derivatives of the nuclear forces with respect to a finite electric field.

A. Interligand Vibrations. The detailed discussion of the interligand vibrations and mode assignment has already been presented in a Letter preceding this publication.[21] The most important interligand vibration is the Co−C_R stretch, which previously has been calculated at 535 cm^{-1} and was obtained based on transferable scaling factors optimized on free base porphine.[20b] Comparison with Raman data shows that these scaling factors have a tendency to overestimate, by approximately 30 cm^{-1}, the experimental values of 506, 504, or 500 cm^{-1}. Taking into account the fact that only a few vibrations have been unambiguously assigned for the corrin-based systems, development of multiple scaling factors based on least-squares fitting of frequencies (see for example ref 13b) is not possible. To improve the agreement between experiment and theory, one scaling factor has been applied and its numerical value optimized by considering: two model systems of Im−[Co^{III}(corrin)]−R with different β axial ligands R = −CH_3 and −CH_2CH_3. For each system, the scaling factor was adjusted to reproduce accurately the Co−C_R stretch frequencies together with their isotope shifts, as well as the most intense corrin modes present in the ∼1500 cm^{-1} spectral range. (The Co−C stretch frequency for the methyl was assumed to be equal to 506 cm^{-1} with 28 cm^{-1} isotope shift for deuterium substitution and 472 cm^{-1} with 20 cm^{-1} deuterium shift for the ethyl. Experimental values were taken from ref 7b.) Interestingly, this new optimal scaling factor was found to have a lower value (0.86) than the comparable single scaling factor for the B3LYP functional (0.93).[13b] This optimal scaling factor for model cobalamins is actually in the range of scaling factors usually used for the force constants calculated on the Hartree−Fock level of theory. The low value of the scaling factor most likely reflects the insufficient treatment of correlation energy and fact that the optimized geometry differs from the actual structure of MeCbl in several points. In particular, the optimized Co−C bond length, 1.96 Å, is 0.03 Å

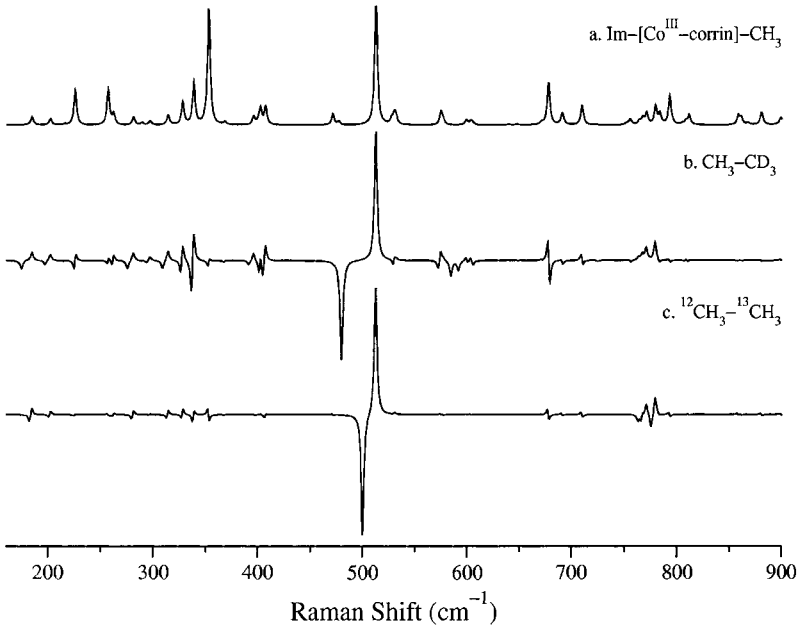

Figure 3. Simulated low frequency (170−900 cm^{-1}) Raman spectrum of Im−[Co^{III}−corrin]−CH_3 from SQM-DFT calculations. (a) Natural abundance, (b) $\Delta(CH_3-CD_3)$ difference spectrum, and (c) $\Delta(^{12}CH_3-^{13}CH_3)$ difference spectrum.

shorter than the experimental value of 1.99 Å. This issue was analyzed and discussed in a previous publication.[17a] The new DFT-SQM force field, based on the improved single scaling factor, gives much better agreement between experiment and theory. The most important interligand vibrations are summarized in Table 1. The new calculated value of the Co−C_R stretch overestimates slightly, i.e., 6 cm^{-1}, the experimental value reported recently by Spiro and co-workers[7] and Marzilli.[9] According to present calculations, this vibration possesses entirely Co−C_R stretch character (88%) without any additional mode mixing. The DFT-SQM force field accurately reproduces isotopic shifts corresponding to the $CH_3 \rightarrow CD_3$ and $^{12}CH_3 \rightarrow {}^{13}CH_3$ isotope substitution (Table 1). The simulated Raman spectrum is shown in Figure 3, together with two difference spectra. The simulated $\Delta(CH_3-CD_3)$ difference spectrum (Figure 4) can be directly compared with resonance Raman data of CH_3Cbl/CD_3Cbl obtained with 530.9 nm laser excitation. Overall, the agreement between the experimental and simulated spectra is remarkable. The theoretical difference spectrum reproduces all spectral features of MeCbl RR spectra very well. In addition to the prominent Co−C_R stretch at 506 cm^{-1}, the band located at 790 cm^{-1} assigned as CH_3 rocking vibration[7b] has a large deuterium shift of ∼200 cm^{-1}. The peak observed at 594 cm^{-1} (Figure 4a) corresponds to its deuterium shift (Table 1). In fact, the 790 and 594 cm^{-1} bands consist of two quasidegenerate vibrations, each due to rocking motions in two orthogonal directions. The Co−CH_3 wagging vibrations (Table 1) cannot readily be identified because they are located in the obscure part of the Raman spectrum in the vicinity of the ice peak (Figure 4a). The old DFT-SQM force field did not confirm vibrational assignment of the 1155 cm^{-1} band,[21] which was reported to shift to 882 cm^{-1} upon deuteration of the methyl group and assigned as asymmetric deformation.[7b] This assignment has to be revised according to the new DFT-SQM force field. The 1155 cm^{-1} band represents symmetric deformation of the Co−CH_3 moiety, which resembles umbrella motion of the three hydrogens with respect to the Co−C bond. The calculated value of 1189 cm^{-1} overestimates the experimental value by 34 cm^{-1}, but the deuterium shift of 277 cm^{-1} is in excellent agreement with experimental value of 273 cm^{-1}

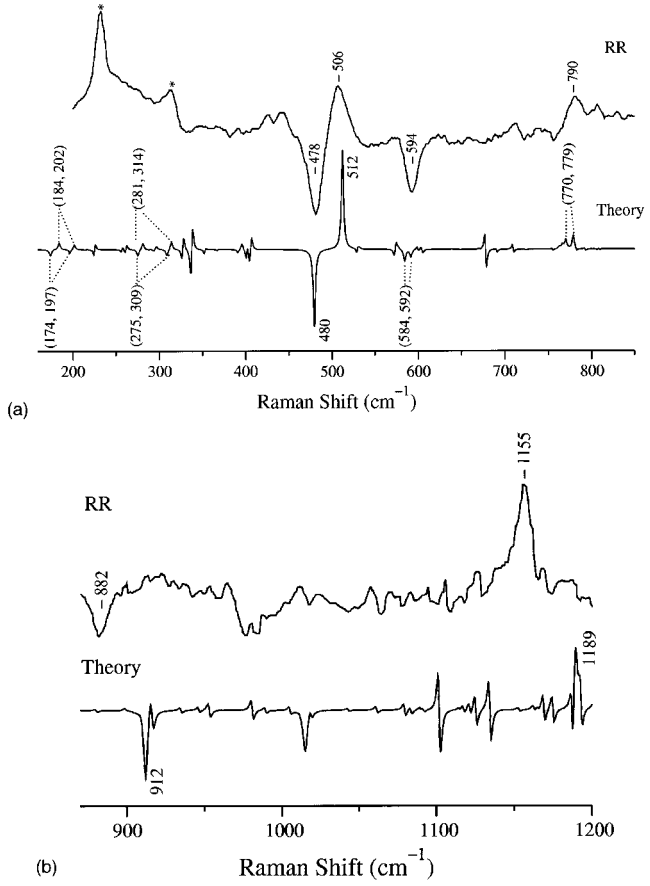

Figure 4. (a) Simulated low-frequency (170−850 cm^{-1}) $\Delta(CH_3-CD_3)$ difference spectrum of Im−[Co^{III}−corrin]−CH_3 based on force field calculations and its comparison with experimental (RR) difference spectrum. The experimental RR spectrum was reproduced from ref 7b. (b) Simulated mid-frequency (870−1200 cm^{-1}) $\Delta(CH_3-CD_3)$ difference spectrum of Im−[Co^{III}−corrin]−CH_3 from SQM-DFT calculations and its comparison with experimental (RR) difference spectrum taken from ref 7b. The negative peak at 1015 cm^{-1} (the positive counterpart of this band is located at 1395 cm^{-1}) corresponds to a scissor motion of the methyl group.

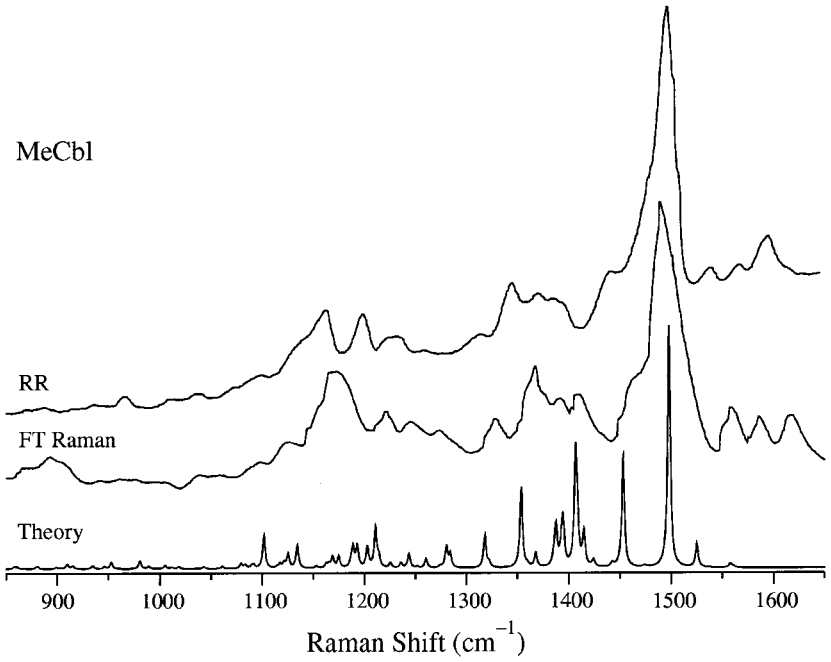

Figure 5. Comparison between the calculated Raman spectrum of Im−[Co^{III}−corrin]−CH_3 and experimental FT-Raman (ref 9a) and RR spectra (ref 7b) in a spectral range of 850−1650 cm^{-1}. Both experimental Raman spectra were numerically digitized and reproduced from original papers. Their alignment to one common scale might be affected by electronic manipulation of digitized data.

(Figure 4b). The 677 and 709 cm^{-1} bands, which show upshift in the difference spectra, are artifacts of the DFT calculations. Both vibrations have dominant corrin character, and both are lightly coupled to $-CH_3$ because of structural simplifications introduced to MeCbl. For completeness of presentation, we have also included simulated IR spectrum for this spectral range (Figure 1S and Figure 2S, see Supporting Information). The Co−C_R stretch has marked IR intensity and can be identified in IR difference spectrum; however, contrary to the Raman spectrum (Figure 3), the most intense IR peak in this spectral range is 527 cm^{-1} and is associated with imidazole vibration.

B. Corrin Modes. As was pointed out in the Introduction, full vibrational assignment for methyl cobalamin represents a difficult problem because the spectrum is congested and selection rules cannot be applied to distinguish nearby modes since the corrin lacks symmetry. Additional complication arises from the fact that the model system (Figure 2) differs from the actual structure of MeCbl, and only selected modes, localized primarily on corrin, can be readily identified and assigned.

The low-frequency part of Raman spectrum contains several modes having off-resonance Raman intensities comparable to the intensity of the Co−C stretch. Table 2 contains these modes with noticeable Raman intensity in the 200−900 cm^{-1} spectral range. (Supporting Information provides the full list of 168 vibrations, together with Raman and IR intensities for Im−[Co^{III}-(corrin)]−CH_3 model.) The majority of these vibrations contain symmetric or asymmetric deformations of the pyrroline rings as well as bending vibrations of the corrin skeleton. The most intense vibration predicted below the Co−C stretch at 353 cm^{-1} is a corrin breathing mode. The calculated value of this mode is in close proximity of the same mode in free base porphine at 304 cm^{-1} [20c] and nickel porphine at 362 cm^{-1}.[16c] Comparison with experimental data suggests that the breathing mode can be correlated with a spectral feature observed near ∼420 cm^{-1}. The 70 cm^{-1} underestimation of this vibration could be a consequence of low scaling, lack of substituents, or combinations of both effects. We tested the possibility that different scaling factors could be applied to vibrations present in this spectral region, but the lack of definitive assignments of corrin modes in this range makes this approach theoretically not well justified.

TABLE 2: Calculated Frequencies [cm^{-1}], Raman Intensities [$(4\pi\epsilon_0)^2$ Å amu^{-1}], Depolarization Ratios, and Total Energy Distributions [%] of Im−[Co^{III}−corrin]−CH_3 Selected Modes in a Spectral Range of 200−900 cm^{-1}

freq.	Raman int.	dep.	description[a]
226	9.0	0.73	$\zeta_{N4,19,1}$ (27), $\zeta_{N1,1,19}$ (21), $\tau_{s,5}$ (11)
257	9.0	0.75	$\zeta_{N4,16,15}$ (16), $\zeta_{N2,9,10}$ (16), $\zeta_{N3,11,10}$ (15), $\zeta_{N3,14,15}$ (14), $\zeta_{N1,4,5}$ (12), $\zeta_{N2,6,5}$ (10)
328	5.8	0.42	$\zeta_{CR,Co,N4}$ (29), $\tau_{s,6}$ (18)
339	11.7	0.21	Co(N_4) oop (12), $\tau_{s,6}$ (7), $\zeta_{N3,11,10}$ (7), $\nu_{9,10}$ (6), $\nu_{10,11}$ (6), $\nu_{11,12}$ (6), $\nu_{8,9}$ (6)
353	30.5	0.12	corrin breathing
402	4.1	0.26	$\zeta_{N2,6,5}$ (19), $\zeta_{N1,4,5}$ (16)
407	4.7	0.09	$\zeta_{N4,16,15}$ (19), $\zeta_{N3,14,15}$ (16)
575	3.4	0.16	ζ_a^A (15), ζ_a^D (11)
677	11.1	0.16	ζ_s^B (10), ζ_s^C (10), ζ_a^B (9), ζ_a^C (10)
709	5.2	0.44	ζ_a^C (12), ζ_a^B (11)

[a] Total energy distributions [%] are given in parentheses; $\zeta_{X,\,Y,\,Z}$, $X-Y-Z$ bendings; $\tau_{s,1}$, $\tau_{s,2}$, ... $\tau_{s,6}$, corrin ring symmetric torsions; $\tau_{a,1}$, $\tau_{a,2}$, ... $\tau_{a,6}$, corrin ring asymmetric torsions; $\nu_{X,Y,X-Y}$ stretch; $\zeta_s^{A,...D}$, symmetric deformation of the pyrolinyl rings (A, B, C, D); $\zeta_a^{A,...D}$, asymmetric deformation of the pyrolinyl rings (A, B, C, D); Co(N_4) oop, Co out of plane motion.

Figures 5 and 6 show a comparison between simulated and experimental FT-Raman and resonance Raman spectra in the 850−1650 cm^{-1} range. Despite the fact that the Im−[Co^{III}-(corrin)]−CH_3 model system (Figure 2) differs from the actual structure (Figure 1), simulated Raman spectra demonstrate the essential vibrational features of MeCbl. Inspection of experimental data (Figures 5 and 6) and normal-coordinate analysis based on SQM-DFT force field suggest that the 850−1650 cm^{-1} spectral range can be divided into four groups of vibrations. The range 850−1100 cm^{-1} represents a relatively flat part of the Raman spectrum for both the CH_3Cbl and CD_3Cbl isotopomers. The DFT calculations indeed show that modes are weak in this region, and ∼20 vibrations have comparable Raman

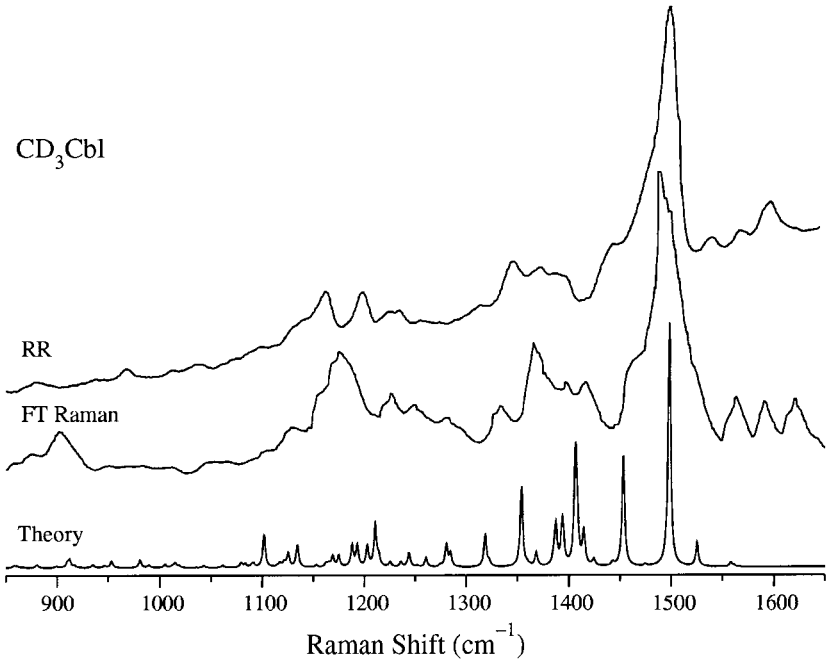

Figure 6. Comparison between the calculated Raman spectrum of Im−[Co^{III}−corrin]−CD_3 and experimental FT-Raman (Reference 9a) and RR spectra (ref 7b) in a spectral range of 850−1650 cm^{-1}. Both experimental Raman spectra were numerically digitized and reproduced from original papers. Their alignment to one common scale might be affected by electronic manipulation of digitized data.

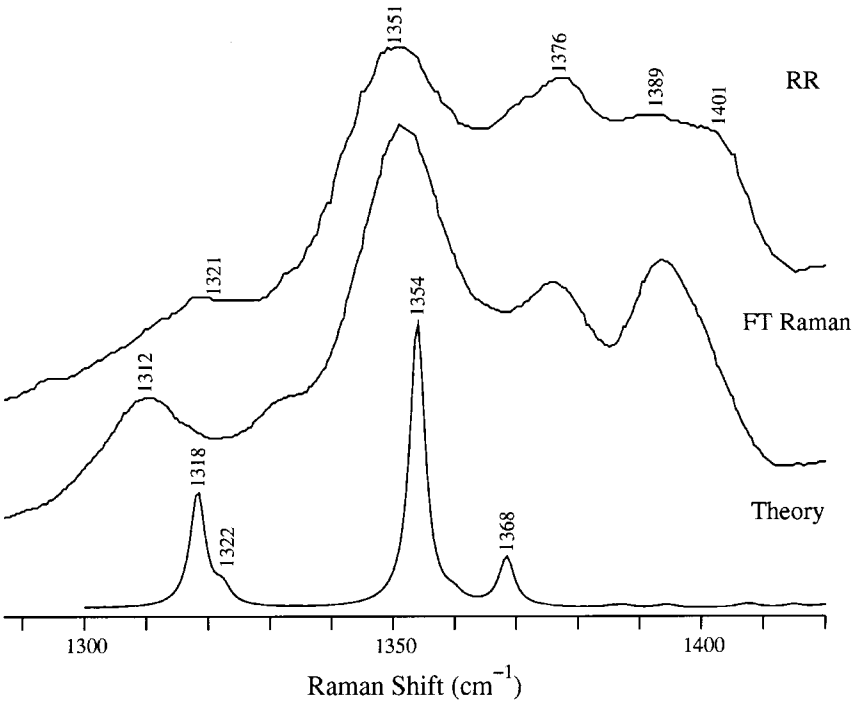

Figure 7. Comparison of calculated Raman spectrum of Im−[Co^{III}−corrin]−CH_3 with the FT-Raman (ref 9b) and RR spectra (ref 7b) in the 1290−1420 cm^{-1} frequency range.

intensities. Dong et al.[7b] marked several RR bands located at 876, 894, 942, 973, 1017, 1044, 1079, and 1102 cm^{-1} with comparable intensities. We have been able to predict several modes in this region at 899, 910, 934, 946, 953, 1018, and 1061 cm^{-1} having frequencies comparable to reported values, but their low Raman intensities make assignment difficult and uncertain. Interestingly, the majority of these calculated vibrations between 900 and 950 cm^{-1} contain C_β−C_β stretch of pyrroline ring as a major component. There are several vibrations near 1167, 1205, 1232, and 1243 cm^{-1}, but they cannot be simply correlated with calculated modes.

The 1300−1400 cm^{-1} RR region of MeCbl contains several bands of medium Raman intensities located at 1321, 1351, 1376, and 1389/1401 cm^{-1} (Figure 7) and 1312, 1351, 1376, and 1393 cm^{-1} in near-IR FT-Raman spectrum of CD_3Cbl, respectively (Figure 7). (Positions of peaks in FT-Raman spectrum has been taken from the digitized spectrum (Figure 7).) In both RR and FT-Raman spectra, the most intense peak of this region is located at 1351 cm^{-1}. The second intense peak at 1376 cm^{-1} present in RR spectrum corresponds exactly to the one observed at 1376 cm^{-1} in FT-Raman. However, the band structure near 1312/1321 and 1390 cm^{-1} is dissimilar in both spectra and the

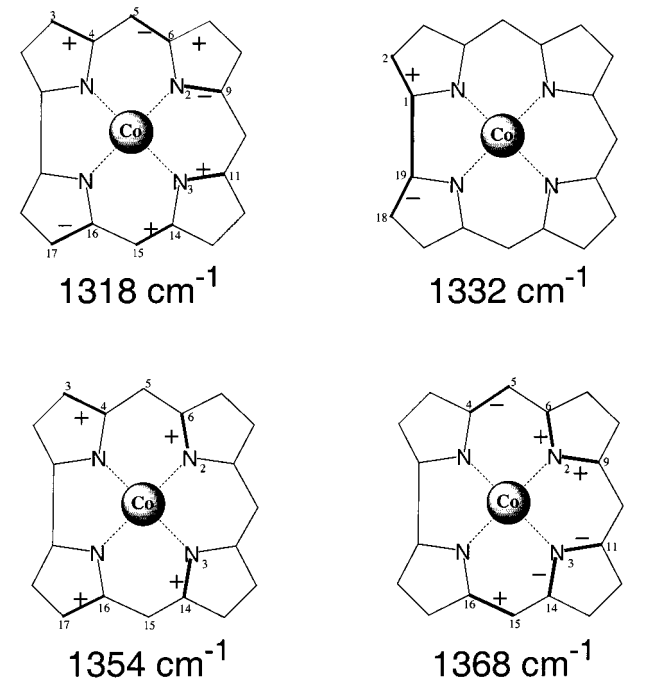

Figure 8. Calculated eigenvectors for 1318, 1332, 1354, and 1368 cm^{-1} corrin modes of Im−[CoIII−corrin]−CH_3. Bold lines represent bond stretch, while signs represent the phase of a particular stretching vibration.

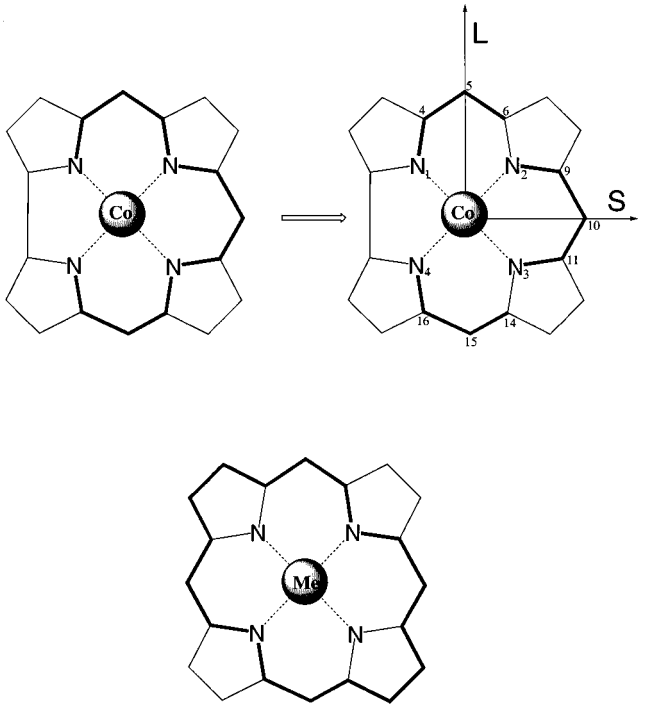

Figure 9. (a) Schematic diagram of the corrin ring framework. The heavy lines show the π-delocalization path. (b) Factorization of the π-delocalization pathway involving corrin vibrations in 1430−1600 spectral region. (c) Schematic diagram of the π-delocalization porphyrin ring framework.

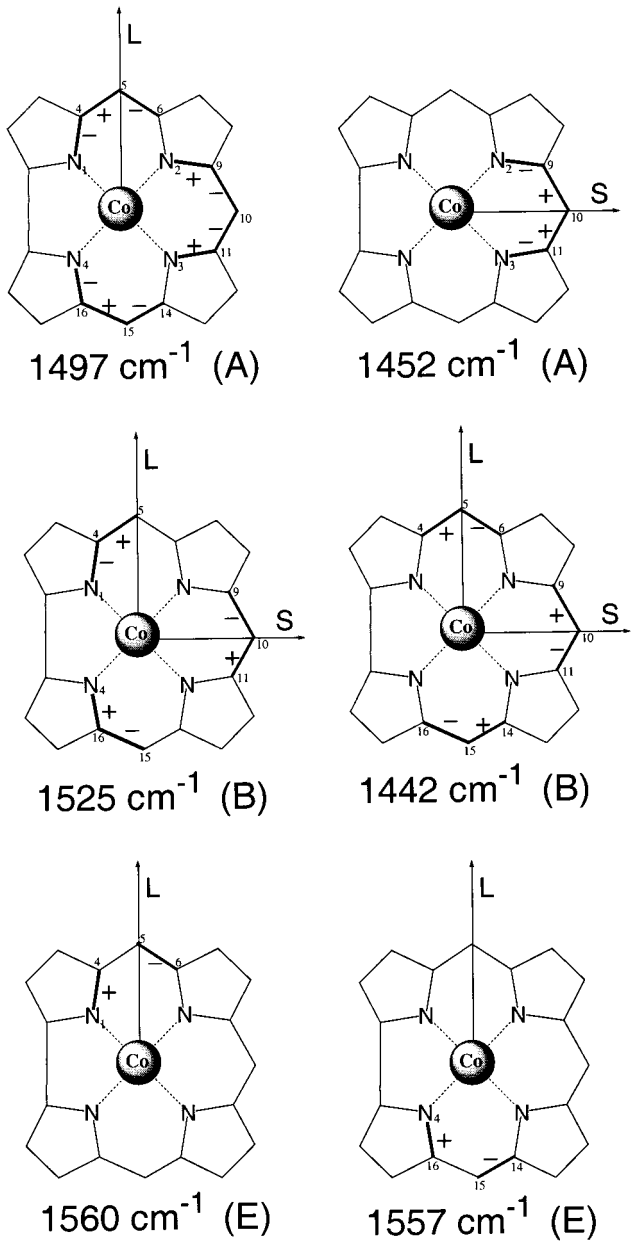

Figure 10. Calculated eigenvectors for 1442, 1452, 1497, 1525, 1557, and 1560 cm^{-1} corrin modes of Im−[CoIII−corrin]−CH_3. Bold lines represent bond stretch, while signs represent the phase of a particular stretching vibration.

intensity pattern differs for the less intense peaks. The pronounced band at 1312 cm^{-1}, which appears only in FT-Raman spectrum, does not have its analogue in RR spectrum. Instead, a broad feature near 1321 cm^{-1} is present in RR (Figure 7). Marzilli and co-workers[9b] noticed that this 1312 cm^{-1} band appears only in CD_3Cbl spectrum but vanishes for the base-off form of CH_3Cbl^+ and CH_3Cbi^+. The presence of this band in $(CN)_2Cbl^-$ and its sensitivity to protonation, but not to coordination, led them to suggest that this band could be assigned as a benzimidazole ring stretching mode.[9b] The band at 1393 cm^{-1} is more intense in FT-Raman than in RR in comparison to 1376 cm^{-1} and does not possess a complex structure as the 1389/1401 cm^{-1} band observed in RR. Spiro and co-workers[7b] noticed several spectral changes in this region which were sensitive to displacement of the DBI axial base. The RR spectra of AdoCbl, which have a similar structure of the high-frequency part to MeCbl recorded at different pH conditions, revealed that the overall enhancement is lower at pH 1.0, that the relative enhancement is diminished for several bands including 1400 cm^{-1}, and that the 1376 cm^{-1} peak shifts to a lower value of 1373 cm^{-1}. The DFT-SQM-based normal-coordinate analysis predicts about 11 modes present in this region (Figures 5 and 6), but some of them have entire hydrogen wagging character due to the simplified character of the model system (Figure 2). To make the comparison with experiment

TABLE 3: Calculated Frequencies [cm^{-1}], Raman Intensities [$(4\pi\epsilon_0)^2$ Å amu^{-1}], Depolarization Ratios, and Total Energy Distributions [%], Together with the Sign Representing the Phase of Stretching Vibration of Corrin Modes in a Spectral Range of 1430−1600 cm^{-1} for Im−[Co^{III}−corrin]−CH_3

freq.	Raman int.	dep.	N1−4	4−5	5−6	N2−9	9−10	10−11	11-N3	14−15	15−16	16-N4
1560	2.0	0.68	33 [+]	0	26 [-]	0	0	0	0	5 [+]	0	0
1557	4.9	0.74	8 [−]	0	0	0	0	0	0	22 [+]	0	39 [−]
1525	29.6	0.75	17 [−]	5 [+]	0	0	14 [−]	14 [+]	0	0	5 [−]	17 [+]
1497	299.1	0.14	10 [−]	8 [+]	13 [−]	6 [+]	0	5 [−]	6 [+]	13 [−]	8 [+]	10 [−]
1452	136.7	0.11	0	0	0	19 [−]	10 [+]	11 [+]	17 [−]	0	0	0
1442	4.9	0.73	0	5 [+]	7 [−]	0	10 [+]	8 [−]	5 [−]	7 [+]	5 [−]	0

possible, we suppressed Raman intensities of modes having large amplitudes on hydrogen atoms, and the remaining vibrations compare directly with Raman spectra (Figure 7). Four corrin modes have been readily identified in this region for which eigenvectors are shown in Figure 8. The most intense mode, calculated at 1354 cm^{-1}, accurately matches the experimental band at 1351 cm^{-1}. This mode primarily involves in-phase, with respect to the Co−C_{10} axis, stretching vibrations of the N_2−C_6 and N_4−C_{14} bonds with contributions from the C_3−C_4 and C_{16}−C_{17} stretches as well (Figure 8). The mode predicted at 1368 cm^{-1} (Figure 8) has a vibrational pattern similar to that of the 1351 cm^{-1} mode, except that the stretching vibrations of the carbon−nitrogen and carbon−carbon bonds are out-of-phase. Consequently, the 1351 cm^{-1} mode has a higher Raman intensity in comparison to its out-of-phase analogue. The intensity ratio of these two modes is comparable to the one observed in the FT-Raman spectrum and suggests that the latter can be assigned to the 1376 cm^{-1} band. There are two modes predicted at 1318 and 1322 cm^{-1}, respectively. The former correlates with 1312 cm^{-1} observed in FT-Raman and the latter with 1321 cm^{-1} present in RR. Interestingly, the calculated mode at 1312 cm^{-1} contains a small contribution from the stretch of the N_B−C bond of the imidazole base, the vibration of which might be sensitive to protonation. This mode is most likely not enhanced in the RR spectrum.

The 1430−1600 cm^{-1} spectral range contains the most distinctive bands of the Raman spectrum located at 1444, 1494, 1544, 1571, and 1600 cm^{-1} (Figures 5 and 6). The DFT-SQM force field for Im−[Co^{III}(corrin)]−CH_3 predicts six in-plane corrin vibrations present in this region. Direct insight into their mode composition shows that they are primarily composed of stretching vibrations of single/double bonds located along the corrin π-delocalization pathway (Figure 9). Figure 10 shows the corresponding eigenvectors while Table 3 summarizes the composition of these modes, i.e., the total energy distribution (TED), together with a sign representing the phase of a particular stretching vibration. The bond stretches which contribute to these six corrin modes are split into three distinct groups of vibrations located along the N_1−C_4−C_5−C_6, C_{14}−C_{15}−C_{16}−N_4 and N_2−C_9−C_{10}−C_{11}−N_3 atoms with negligible contribution from the C_6−N_4 and N_3−C_{14} stretching vibrations (Table 3 and Figure 10). The alignment of the first two groups is along the longer C_5−Co−C_{15} axis, while the third is along the shorter C_{10}−Co axis of the corrin ring (Figure 10). The most intense Raman mode, calculated at 1497 cm^{-1}, is composed of in-phase stretching vibrations of the double C=C bonds along the long axis of the corrin π system (Table 3 and Figure 10). The second most intense 1452 cm^{-1} corrin mode involves in-phase stretching vibrations of the double C=C bonds along the shorter axis of the corrin macroring. The two modes predicted at 1525 and 1442 cm^{-1} involve the out-of-phase combinations of single/double bond stretching vibrations essentially distributed over the π-conjugation pathway. Their distribution pattern looks somewhat similar, though stretches of the 1525 cm^{-1} mode are localized primarily on the N_1−C_4 and N_4−C_{16} bonds while for

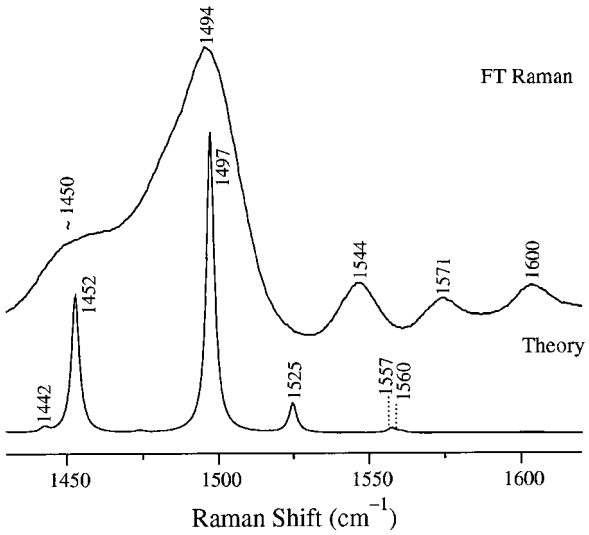

Figure 11. Comparison of calculated Raman spectrum of Im−[Co^{III}−corrin]−CH_3 with the FT-Raman spectrum (ref 9b) in the 1425−1625 cm^{-1} frequency range.

1442 cm^{-1} on C_5−C_6 and C_{14}−C_{15}. The two highest vibrations predicted at 1560 and 1557 cm^{-1} possess an essentially degenerate character. They differ only by about 3 cm^{-1}, and both of them contain out-of-phase stretch of CC double bonds. These two out-of-phase stretches are located along the longer corrin axis, in the upper and lower part of the corrin macroring aligned with respect to the *L* axis (Figure 10).

Direct comparison of the simulated off-resonance Raman spectrum in the ~1450−1600 cm^{-1} spectral range with non-resonant FT-Raman data (Figure 11) shows semiquantitative agreement between experiment and theory. The most intense mode predicted at 1497 cm^{-1} exactly matches the most intense Raman band at 1494 cm^{-1}. This exact correspondence is a consequence of the scaling procedure applied to DFT force constants. It was pointed out before that two reference bands, i.e., the Co−C stretch and the above corrin mode, were used to adjust calculated and experimental spectra. This band has a multicomponent structure, and according to current DFT calculations, two additional corrin modes predicted at 1442 and 1452 cm^{-1} could be considered as part of this intense band. The vibration at 1442 cm^{-1} has a very low Raman intensity, but the mode predicted at 1452 cm^{-1} correlates nicely with the spectral feature observed near 1450 cm^{-1}. The calculated intensity ratio of the 1497 and 1452 cm^{-1} modes additionally supports this assignment. The assignment of the three remaining corrin modes is somewhat problematic. The 1525 cm^{-1} mode can be assigned to 1544 cm^{-1} and the pair of 1557/1560 cm^{-1} to the peak observed at 1571 cm^{-1}. The other possibility is to assign the pair of 1557/1560 cm^{-1} vibrations to 1544 cm^{-1} and assume that the 1525 cm^{-1} mode is hidden under the intense 1494 cm^{-1} band. Present DFT calculations do not provide any reasonable explanation for the band present at 1600 cm^{-1}.

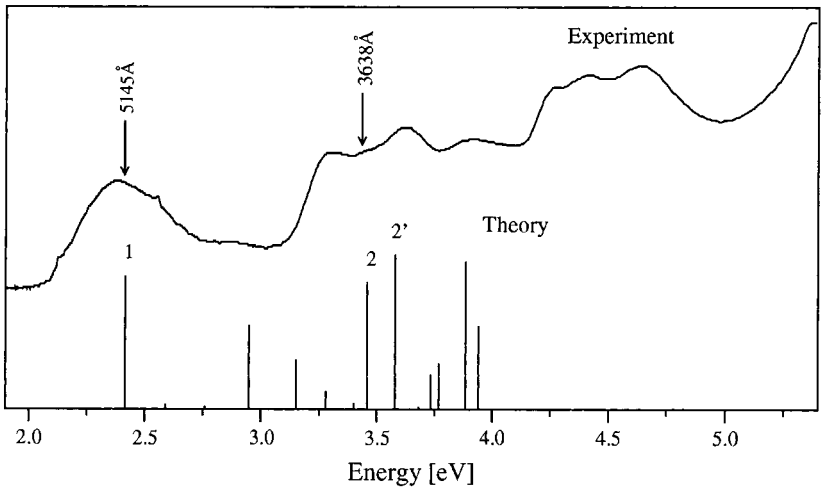

Figure 12. Comparison between the TD-DFT electronic excitation spectra for Im−[Co^{III}−corrin]−CH_3 and the experimental absorption spectrum (ref 7b) in a range of 2.0−4.0 eV. Arrows indicate the laser excitation energies used in RR experiment.

This interpretation of the most intense Raman bands only partly agrees with the assignment proposed by Salama and Spiro.[11] The band at 1496 cm^{-1} and the one at 1545 cm^{-1} have been assigned as in-phase stretching of the double bond along the longer axis (*L*) and the shorter (*S*) axis of the corrin ring, respectively (Figure 10). These assignments were based on selective enhancement of one band with visible light (5145 Å) and the other by near-UV light (3638 Å). The two different $\pi \rightarrow \pi^*$ corrin transitions associated with each electronic absorption band are known to be polarized along one of these axes. The decrease of in-phase double-bond stretching modes in polyenes with increasing chain length supported the assignment to the corrin long and short modes.[22] The assignment of the corrin mode along the long axis agrees exactly with the description proposed by Salama and Spiro, but assignment of the mode along the short axis differs the from assignment discussed above. To investigate this assignment further, we calculated the first 15 excited states of Im−[Co^{III}(corrin)]−CH_3 using time-dependent DFT and compared them with the experimental absorption spectrum (Figure 12).[7b] The calculated electronic transitions in the range 2.0−4.0 eV accurately agree with the experimental absorption spectrum. Immediate comparison of experimental and theoretical data suggests that the band near 5145 Å resembles the Q-band observed in porphyrins while the one near 3638 Å resembles the intense B or Soret band. Closer analysis of the excited states suggests that the excited states of corrin are more in line with those observed in phthalocyanines rather than those in porphyrins. The analysis of corrin excited states will be discussed in a future publication.[12] The main point of these calculations is the appearance of the electronic transition near 5145 Å (labeled as 1) which has a transition moment aligned along the long axis (*L*). There are two electronic transitions near 3638 Å (labeled as 2 and 2′) with transition dipole moments aligned along the short corrin axis (Figure 13). The alignment of transition dipole moments as well as mode composition of corrin vibrations based on DFT calculations support the assignments suggested by Salama and Spiro[11] a long time ago. The problem occurs with the calculated frequency of this short mode, which after scaling is equal to 1452 cm^{-1}, rather than being in the vicinity of 1550 cm^{-1}. In the near-UV RR spectrum, the most intense peak is ∼1550 cm^{-1}, which corresponds to 1544 cm^{-1} in the FT-Raman spectrum (Figure 11). We have proposed two plausible assignments of the 1544 cm^{-1} band, but neither of them correspond to in-phase along the short corrin axis. It is unlikely that the

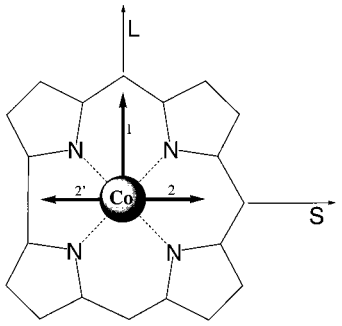

Figure 13. Alignment of the transition dipole moment representing electronic transition near 5145 (1) and 3638 Å (2,2′).

replacement of substituents by hydrogen atoms would result in the underestimation of this frequency by 100 cm^{-1}, especially since this mode has a rather localized character and should not be influenced by the nature of peripherial substituents. The other possibility is that a different mode is actually enhanced in near-UV RR. This is a plausible interpretation if one takes into account the pseudo-symmetry of these six corrin modes. The 1497 and 1452 cm^{-1} modes can be viewed as totally symmetric *A* modes, the two vibrations at 1525 and 1442 cm^{-1} as *B*, while the pair of 1560/1557 cm^{-1} as degenerate vibrations of symmetry *E*. This analysis has only a qualitative meaning, but illustrates the point that regardless of the enhancement mechanism the different pairs of vibrations should be enhanced together. Marzilli and co-workers[9b] pointed out that the ∼1544 cm^{-1} band is sensitive to base replacement. The slight difference in frequency of this band was attributed to the different ligand electron-donor abilities, and it was suggested that this might be indicative of secondary structural effects. Our present calculations were not able to prove or disprove this hypothesis because only one ligand (Im) was used in vibrational analysis. All of these facts make assignment of this range rather uncertain; more elaborate experiments and theoretical studies are required to solve these existing ambiguities.

Summary and Conclusion

This work represents first theoretical effort to assign vibrational modes for methylcobalamin, a biologically active form of vitamin B_{12}. To accomplish this a reliable structural model, which includes the actual corrin ring (Figure 2), was used in vibrational calculations. The normal-coordinate analysis, based

on DFT-SQM force field predicts accurately all interligand vibrations but gives only semiquantitative description of corrin modes. The calculated vibrations and their off-resonance Raman intensities capture the essential spectral features of MeCbl. The comparison of Raman data with DFT computed vibrations allowed only for the assignment of certain vibrations located in the 1300−1600 cm^{-1} spectral range. The complexity associated with vibrational assignment arose mainly from the fact that vibrational spectra are congested and a majority of the modes have low Raman intensities. Additional complications to vibrational analysis introduce uncertainty to the direct comparison of experimental data with calculated caused by structure simplification. This study clearly demonstrates that the full vibrational analysis of MeCbl represents a complex and difficult problem. Two factors can change this situation in future. More complete spectroscopic data obtained for several isotopomers combined with infrared and multiple wavelength resonance Raman studies would allow us to distinguish nearby modes. On the other hand, more reliable structural models employed in DFT calculations would be required to obtain better agreement with experiment.

Despite the aforementioned problems related to assignment, current theoretical studies provide valuable insight into the vibrational structure of the corrin macrocycle. Although corrin is somewhat similar to porphyrin, the vibrational modes of these two systems have quite different structures. The $C_\beta-C_\beta$ stretching vibration is one of the major contributors to metalloporphyrins' most intense Raman bands. For example, vibrations observed at 1459, 1505, and 1574 cm^{-1} denoted as ν_3, ν_{11}, and ν_2, respectively, dominate the FT-Raman spectrum of nickel porphine near 1500 cm^{-1}.[16c] These three modes possess significant contributions from the $C_\beta-C_\beta$ stretch, being equal to 56%, 68%, and 27%, respectively. Contrary to porphyrins, the most intense Raman corrin modes near 1500 cm^{-1} have negligible contributions from the $C_\beta-C_\beta$ stretches. According to present DFT-based calculations, the majority of modes having significant $C_\beta-C_\beta$ stretch involvement were actually predicted at much lower frequencies ~900−950 cm^{-1} with very low Raman intensity. This low Raman intensity of $C_\beta-C_\beta$ is a consequence of the corrin ring being partially saturated, containing pyrrolines instead of pyrroles. In principle, the different vibrational pattern of the corrin macrocycle in comparison to porphyrin in the 1300−1600 spectral range has its origin in the different electronic structures of these two systems. In the case of porphyrins, the $C_\beta-C_\beta$ bonds participate in the 18-member ring of the π-delocalization pathway[20b] (Figure 9), while in corrin, the π-delocalization pathway does not contain any $C_\beta-C_\beta$ bonds. The π-delocalization pathway in corrin involves 12 single/double bonds (Figure 9), which does not fulfill the $4n + 2$ Huckel rule. The factorizations of vibrations in the 1450−1600 cm^{-1} range (Figure 9) reflect somehow the tendency of the corrin ring to be "aromatic". This is pronounced by the lack of involvement of the two stretching CN vibrations in corrin's most intense bands. In general, vibrations of the corrin ring have localized character in comparison to porphyrins. These modes resemble more the vibrations of connected short linear polyenes rather than modes delocalized over the corrin ring. Most likely this localized character is responsible for lack of structure-sensitive modes such as the "core size" marker as has been concluded in earlier RR studies of B_{12}.[11]

Supporting Information Available: Full list of 168 vibrations of Im−[Co^{III}−corrin]−CH_3 derived from SQM-DFT analysis, together with IR intensities, dipole moments, Raman intensities, depolarization ratios and IR spectra. This material is available free of charge via the Internet at http://pubs.acs.org.

References and Notes

(1) (a) Dolphin, D., Ed. In *B_{12}*; Wiley−Interscience: New York, 1982. (b) Kräutler, B., Arigoni, D., Golding, B. T., Eds. In *Vitamin B_{12} and B_{12}-Proteins*; Wiley-VCH: New York, 1998.

(2) Kräutler, B., Arigoni, D., Golding, B. T., Eds. In *Vitamin B_{12} and B_{12}-Proteins*; Wiley-VCH: New York, 1998; Chapter IV.

(3) Stubbe, J.; Llicht, S.; Gerfen, G.; Silva, D.; Booker, S. In *Vitamin B_{12} and B_{12}-Proteins*; Kräutler, B., Arigoni, D., Golding, B. T., Eds.; Wiley-VCH: New York, 1998.

(4) Kräutler, B., Arigoni, D., Golding, B. T., Eds. In *Vitamin B_{12} and B_{12}-Proteins*; Wiley-VCH: New York, 1998; Chapter III.

(5) Spiro, T. G., Ed. In *Biological Applications of Raman Spectroscopy*; Wiley-VCH: New York, 1998.

(6) Ervin, A. M.; Shupack, S. I.; Byler, D. M. *Spectrosc. Lett.* **1984**, *17*, 603.

(7) (a) Dong, S.; Padmakumar, R.; Banerjee, R.; Spiro, T. G. *J. Am. Chem. Soc.* **1996**, *118*, 9182. (b) Dong, S.; Padmakumar, R.; Banerjee, R.; Spiro, T. G. *Inorg. Chim. Acta* **1998**, *270*, 392.

(8) Dong, S.; Padmakumar, R.; Banerjee, R.; Spiro, T. G. *J. Am. Chem. Soc.* **1999**, *121*, 7063.

(9) (a) Nie, S.; Marzilli, P. A.; Marzilli, L. G.; Yu, N.-T. *J. Chem. Soc. Chem. Commun.* **1990**, 770. (b) Puckett, J. M.; Mitchell, M. B.; Hirota, S.; Marzilli, L. G. *Inorg. Chem.* **1996**, *35*, 4656.

(10) (a) Wozniak, W. T.; Spiro, T. G. *J. Am. Chem. Soc.* **1973**, *95*, 3402. (b) Mayer, E.; Gardiner, D. J.; Hester, R. E. *Mol. Phys.* **1973**, *26*, 783. (c) Mayer, E.; Gardiner, D. J.; Hester, R. E. *J. Chem. Soc., Faraday Trans. 2* **1973**, *69*, 1350. (d) Galuzzi, F.; Garozzo, M.; Ricci, F. F. *J. Raman Spectrosc.* **1974**, *2*, 351.

(11) Salama, S.; Spiro, T. G. *J. Raman Spectrosc.* **1977**, *6*, 57.

(12) Andruniow, T.; Zgierski, M. Z.; Kozlowski, P. M. Manuscript in preparation.

(13) (a) Pulay, P.; Fogarasi, G.; Pongor, G.; Boggs, J. E.; Vargha, A. *J. Am. Chem. Soc.* **1983**, *105*, 7037. (b) Rauhut, G.; Pulay, P. *J. Phys. Chem.* **1995**, *99*, 3093.

(14) Frisch, M. J.; Trucks, G. W.; Schlegel, H. B.; Scuseria, G. E.; Robb, M. A.; Cheeseman, J. R.; Zakrzewski, V. G.; Montgomery, J. A., Jr.; Stratmann, R. E.; Burant, J. C.; Dapprich, S.; Millam, J. M.; Daniels, A. D.; Kudin, K. N.; Strain, M. C.; Farkas, O.; Tomasi, J.; Barone, V.; Cossi, M.; Cammi, R.; Mennucci, B.; Pomelli, C.; Adamo, C.; Clifford, S.; Ochterski, J.; Petersson, G. A.; Ayala, P. Y.; Cui, Q.; Morokuma, K.; Malick, D. K.; Rabuck, A. D.; Raghavachari, K.; Foresman, J. B.; Cioslowski, J.; Ortiz, J. V.; Stefanov, B. B.; Liu, G.; Liashenko, A.; Piskorz, P.; Komaromi, I.; Gomperts, R.; Martin, R. L.; Fox, D. J.; Keith, T.; Al-Laham, M. A.; Peng, C. Y.; Nanayakkara, A.; Gonzalez, C.; Challacombe, M.; Johnson, P. B.; Chen, W.; Wong, M. W.; Andres, J. L.; Gonzalez, C.; Head-Gordon, M.; Replogle, E. S.; Pople, J. A. *Gaussian 98*, Revision A.3; Gaussian, Inc.: Pittsburgh, PA, 1998.

(15) 5 Schaefer, A.; Horn, H.; Ahlrichs, R. *J. Chem. Phys.* **1992**, *97*, 2571.

(16) (a) Kozlowski, P. M.; Spiro, T. G.; Berces, A.; Zgierski, M. Z. *J. Phys. Chem. B* **1998**, *102*, 2603. (b) Spiro, T. G.; Kozlowski, P. M.; Zgierski, M. Z. *J. Raman Spectrosc.* **1998**, *29*, 869. (c) Kozlowski, P. M.; Rush, T. S., III; Jarzecki, A. A.; Zgierski, M. Z.; Chase, B.; Piffat, C.; Ye, B.-H.; Li, X.-Y.; Pulay, P.; Spiro, T. G. *J. Phys. Chem.* **1999**, *103*, 1357. (d) Rush, T. S., III; Kozlowski, P. M.; Piffat, C. A.; Kumble, R.; Zgierski, M. Z.; Spiro, T. G. *J. Phys. Chem. B* **2000**, *104*, 5020. (e) Jarzecki, A. A.; Kozlowski, P. M.; Pulay, P.; Ye, B.-H.; Li, X.-Y. *Spectrochem. Acta, A* **1997**, *53*, 1195.

(17) (a) Andruniow, T.; Zgierski, M. Z.; Kozlowski, P. M. *J. Phys. Chem. B* **2000**, *104*, 10921. (b) Andruniow, T.; Zgierski, M. Z.; Kozlowski, P. M. *Chem. Phys. Lett.* **2000**, *331*, 509. (c) Andruniow, T.; Zgierski, M. Z.; Kozlowski, P. M. *J. Am. Chem. Soc.* **2001**, *123*, 2679.

(18) , Fogarasi, G.; Zhou, X.; Taylor, P. W.; Pulay, P. *J. Am. Chem. Soc.* **1992**, *114*, 8191.

(19) Pulay, P. *TX90*; Fayetteville, AR, 1990. Pulay, P. *Theor. Chim. Acta* **1979**, *50*, 229.

(20) (a) Kozlowski, P. M.; Zgierski, M. Z.; Pulay, P. *Chem. Phys. Lett.* **1995**, *247*, 379. (b) Kozlowski, P. M.; Jarzecki, A. A.; Pulay, P. *J. Phys. Chem.* **1996**, *100*, 7007. (c) Kozlowski, P. M.; Jarzecki, A. A.; Pulay, P.; Li, X.-Y.; Zgierski, M. Z. *J. Phys. Chem.* **1996**, *100*, 13985.

(21) Andruniow, T.; Zgierski, M. Z.; Kozlowski, P. M. *Chem. Phys. Lett.* **2000**, *331*, 502.

(22) Gavin, R. M.; Rice, S. A. *J. Chem. Phys.* **1971**, *55*, 2675.